



COBALT (II) REMOVAL FROM AQUEOUS SOLUTIONS BY ADSORPTION ONTO MOLECULAR SIEVES

**G. BABU RAO^{*,a}, M. KRISHNA PRASAD^a and
Ch. V. R. MURTHY^b**

^aDepartment of Chemical Engineering, GMR Institute of Technology,
RAJAM – 532127, Dist.: Srikakulam (A.P.) INDIA

^bDepartment of Chemical Engineering, University College of Engineering, Andhra University,
VISAKHAPATNAM – 530003 (A.P.) INDIA

ABSTRACT

Cobalt is a heavy metal that is commonly used in industrial processes and used in batteries and tanning activities. Time-dependent experiments were carried out to study the adsorption kinetics of cobalt (II) ions onto 3 Å molecular sieves in batch conditions at room temperature. The influence of contact time, initial solution pH, initial cobalt (II) concentration, adsorbent dosage and temperature was studied in batch experiments. The experimental data was fitted to pseudo-first (Lagergren model) and pseudo-second order kinetics. According to the modelling, experimental data is better resembled to the pseudo-second order kinetics as shown by its correlation coefficient, indicating that 6 hrs are needed to reach equilibrium. The adsorption data were confronted by using both Langmuir and Freundlich classical adsorption isotherms. The experimental data fitted the Freundlich isotherm from the correlation coefficients.

Key words: Adsorption, Free energy change, Cobalt (II), 3Å Molecular sieves FTIR, SEM.

INTRODUCTION

Industries like battery manufacture, metal plating, mining, pigment dye stuff, and chemical industries discharge many heavy metal ions into industrial waste waters¹. These are unintentionally disposed into nearby water bodies or unused and barren tracts of land; thereby, giving rise to severe environmental contamination or degradation. In majority of instances, the metal-bearing effluents contain a wide range of noble metals as well as harmful and hazardous metals such as Ag, Al, Cd, Co, Cr, Cu, Fe, Mg, Mn, Ni, Pb, Sr and

* Author for correspondence; E-mail: baburao01803@gmail.com

Zn. All these metals are non-degradable and thus persistent in their nature². Cobalt exists in the form of various salts in the environment and is widely used in the nuclear medicine, enamels, and semiconductors, painting on glass and porcelain, paint and varnish industries, as a foam stabilizer in beer and as catalyst in organic chemical reactions. The permissible limit of cobalt in irrigation and potable water is 0.05 and 1.0 mg L⁻¹, respectively. High concentration of cobalt causes low blood pressure, mutagenesis, diarrhoea, lung irritation and bone defects^{3,4}.

EXPERIMENTAL

Material and methods

Selection of adsorbent

Molecular Sieves⁵ or zeolites are crystalline aluminum silicates of group IA and IIA elements used for the separation. Zeolites selectively adsorb or reject molecules based upon differences in their size, shape and other properties such as polarity. These are supplied as pellets, granules or beads and occasionally powders. These adsorbents are regenerated and may be re-used. The pore size of the molecular sieves was found to significantly affect the metal ion distribution.

Preparation of stock solution

Cobalt chloride solution was prepared by dissolving 3.617 g cobalt chloride salt in 1000 mL standard volumetric flask with de-mineralized water. The primary stock solution thus prepared gave approximately 2000 ppm of Co²⁺ in solution. From the stock solutions, experimental test solutions were prepared by diluting the primary stock solution with de-mineralized water. The pH range was adjusted by rational addition of specified mineral acid.

Equilibrium studies

The experiments were carried out in 250 mL Erlenmeyer conical flasks, at a constant agitation speed (160 rpm) with 100 mL solution and required amount of adsorbent using orbital shaker (Kemi make). Initially the effect of contact time (0-360 min) on the sorption capacity of 3Å molecular sieves was evaluated. The equilibrium time was obtained and the experiments were conducted for the same time for all conditions. Batch experiments were carried out to investigate the adsorption behavior of Co²⁺ on 3Å molecular sieve.

Analysis of heavy metal ions

The concentrations of unadsorbed Co^{2+} , in the sample solutions were determined using an Atomic Absorption Spectrophotometer (Perkin-Elmer model AA 400). The metal uptake (q_e) was calculated using the general definition:

$$q_e = \frac{V \times (C_T - C_e)}{M} \quad \dots(1)$$

where q_e is the metal uptake of $\text{mg Co}^{2+} \cdot \text{g}^{-1}$ adsorbent, V is the volume of metal containing solution in contact with the adsorbent in L, C_T and C_e are the total and equilibrium (residual) concentration of metal in the solution mg L^{-1} , respectively, and M is the amount of added biosorbent in g.

Metal % of removal by 3Å molecular sieves was determined by Eq. (2) as follows:

$$R (\%) = (C_T - C_e) / C_T \times 100 \quad \dots(2)$$

where R is the percentage of Co (II) adsorbed by biomass, C_T is the total concentration of metal ions in mg L^{-1} and C_e is the concentration of metal ions at time t in mg L^{-1} .

Characterization of biomass

FTIR studies

The powdered biomass, prior and after adsorption was air dried, and demineralized at 60°C in humidity control oven. The powder was analyzed by Fourier transform infra red spectrophotometer. FTIR studies were conducted by potassium bromide (KBr) pellet method (Jasco 5300) in the wave number range of $400.00\text{-}4000.00 \text{ cm}^{-1}$.

Scanning electron microscopy

The dried bio mass powders and the corresponding metal ion loaded powders were coated with ultra-thin film of gold by an ion sputter (JFC-1100), exposed under electron microscope (JEOL, JX-8100) at working height of 15 mm with voltage ranging between 10 and 25 kV.

RESULTS AND DISCUSSION

Effect of contact time

The effect of contact time on % adsorption of each metal Co^{2+} was studied independently over a time period of 6 hrs using different amounts of adsorbent and 100 mL of aqueous solution containing 140 ppm of the metal ion at pH 5 and at temperature 298 K. The experimental data have been plotted as a variation of aqueous metal concentration with time (Fig. 1). It can be observed from the graph that the metal ion concentration decreases with time and reaches a plateau after 5½ for Co^{2+} using 3 Å molecular sieves, indicating attainment of equilibrium. No significant changes in the adsorption with further increase in contact time was noticed.

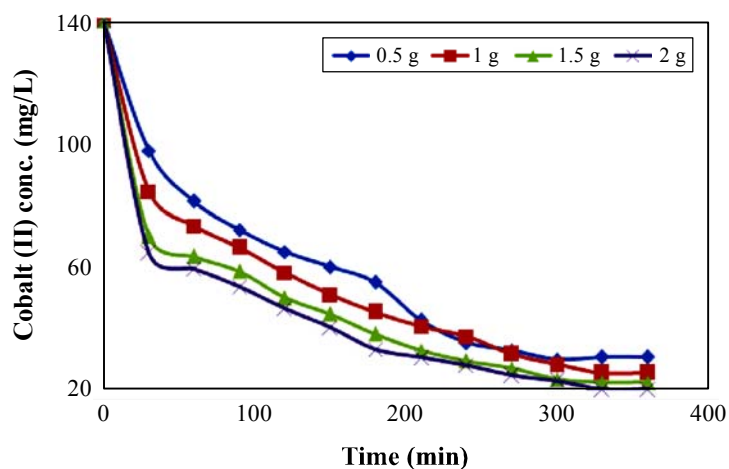


Fig. 1: Variation of aqueous metal (Co^{2+}) concentration with time using 3Å molecular sieves as an adsorbent at 25°C, 141 mg L⁻¹ and pH 5

Effect of pH

The effect of pH on the adsorption of Co^{2+} metal ion over 3 Å molecular sieves were studied in the pH range 3-6. The percent removal of adsorption was increased from 51.84% to 64.84% (Fig. 2) at a total metal ion concentration of 48 mg L⁻¹ as pH was increased from 3 to 5. The maximum adsorption was found to be 60.85% at pH 5 and therefore, all the subsequent experiment runs were conducted at pH 5. At pH beyond 5, the adsorption yield for Co^{2+} ions showed a decline. Similar behavior was reported by different authors⁶⁻¹⁰ while using activated carbon, kaolinite and low-grade phosphate, bone char and activated carbon

of coconut shell as adsorbents. Further increase in pH, decreases the metal adsorption as discussed for Co^{2+} .

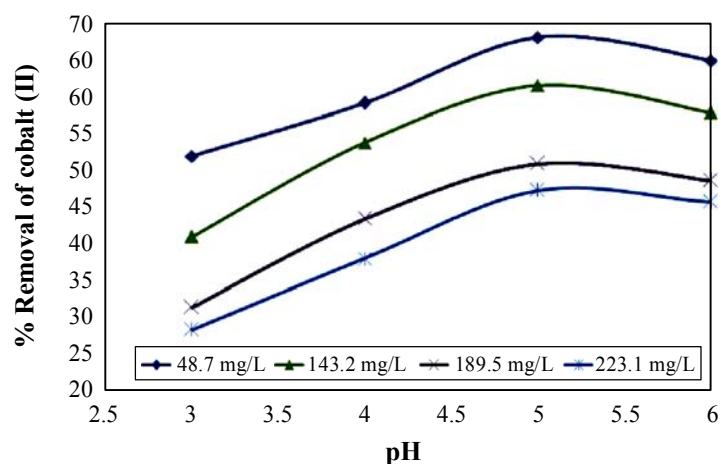


Fig. 2: Effect of pH on percent adsorption at various total metal ion (Co^{2+}) concentrations and at a temperature of 25°C and 20 g L^{-1} , using 3\AA molecular sieves

Effect of metal ion concentration

The increase in total Co^{2+} concentration from 48.75 g L^{-1} to 223.14 mg L^{-1} decreased the percent of removal from 68.02% to 47.12% (Fig. 3) at a sorbent dosage of 20 g L^{-1} , temperature 25°C and pH 5 using 3\AA molecular sieves.

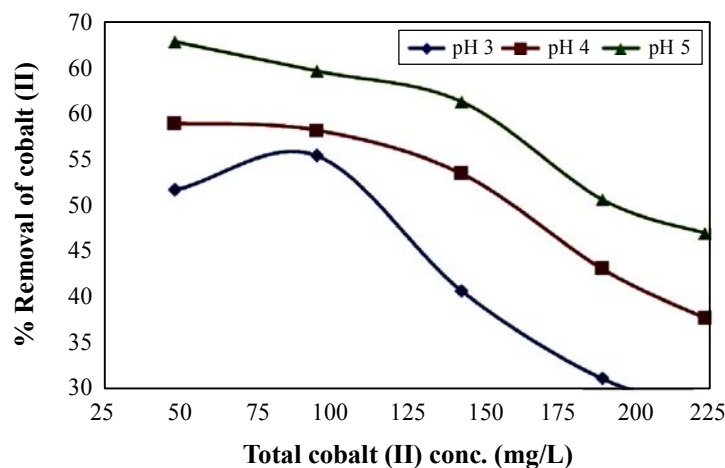


Fig. 3: Variation of % removal of Co^{2+} with various total concentration of Co^{2+} at temperature of 25°C , 20 g L^{-1} of 3\AA molecular sieves

This can be attributed to the reasons cited above that, further available sorption sites on the 3 Å molecular sieves were found to be limited. The adsorption capacity (q_e) of the biomass increased with increasing Co^{2+} initial concentration. An increase in the initial ion concentration provides a larger driving force to overcome all mass transfer resistances between the solid and the aqueous phase, which results in higher metal ion adsorption.

Effect of adsorbent dosage

The effect of adsorbent dosage on the adsorption of Co^{2+} metal ions is shown in following Figs. The biomass dosage has been varied from 5 to 20 g L^{-1} of adsorbate.

The following observations can be made from the plots of the data. The total concentrations of metal ions (Co^{2+}) have been maintained in the range of 24 to 237 mg L^{-1} using 3 Å molecular sieves.

It can be observed from Fig. 4, that the % removal of Co^{2+} for 3 Å molecular sieves, were increased from 37.87 to 68.03% at a pH value of 5, while the uptake capacity showed a decrease from 3.69 to 1.66 mg g^{-1} as the adsorbent weight increases from 5 to 20 g L^{-1} at a total Co^{2+} Concentration of 48 mg L^{-1} (Fig. 5).

Adsorbent dosage determines the potential of adsorbent through the number of binding sites available to remove metal ions at a specified initial metal ion concentration. The increase in percent adsorption of metals by increasing the biomass dosage is due to an increase in the number of active sites and surface area available for adsorption.

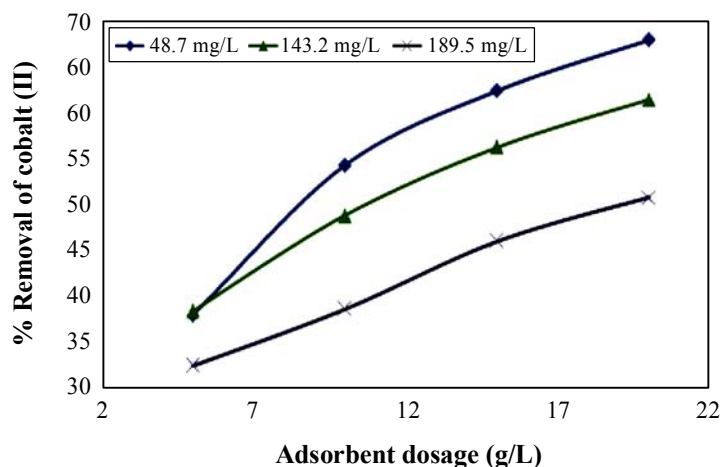


Fig. 4: Variation of % Co^{2+} adsorption with various adsorbent weights of various total metal ion concentration at temp of 25°C and pH 5, using 3 Å molecular sieves

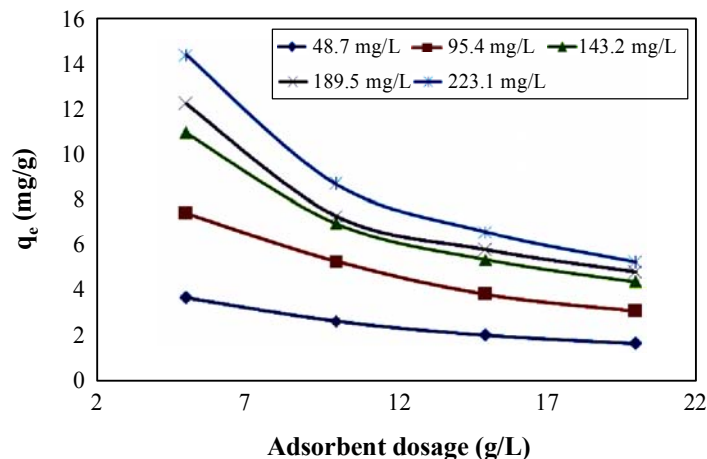


Fig. 5: Variation in metal ion uptake (q_e) of % Co^{2+} adsorption various adsorbent weights at temp of 25°C and pH 5, using 3 \AA molecular sieves

Effect of temperature

The effect of temperature on % removal of metal ions (Co^{2+}) over 3 \AA molecular sieves was shown in Fig. 6. All the experiments with Co^{2+} were conducted in the temperature range of $15\text{-}40^\circ\text{C}$. The capacity of Co^{2+} adsorption by 3 \AA molecular sieves increased from 58.13 to 64.82% with an increase in temperature in the range $15\text{-}40^\circ\text{C}$ (see at a total concentration of 100 mg L^{-1}). It may be due to the rise in temperature, which has a tendency to desorb the adsorbed metal ions from the interface to the solution.

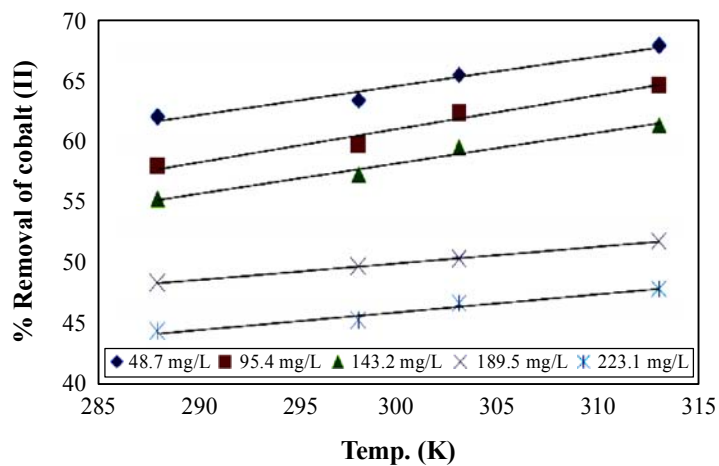


Fig. 6: Variation of percent adsorption of Co^{2+} metal ion with temperature using 3 \AA molecular sieves as adsorbent at different total metal ion concentrations and at pH 5

Adsorption isotherm models

The Langmuir and Freundlich equations are commonly used for describing adsorption equilibrium of adsorbate onto the adsorbent. The Langmuir isotherm is applicable to monolayer chemisorptions while Freundlich isotherm is used to describe adsorption on surface having heterogenous energy distribution:

Langmuir isotherm

A basic assumption of the Langmuir theory is that sorption takes place at specific homogeneous sites within the sorbent. This model can be written in non-linear form and is represented by the equation:

$$\frac{C_e}{q_e} = \frac{1}{q_m b} + \frac{C_e}{q_m} \quad \dots(3)$$

where q_m is the maximum amount of the metal ion per unit weight of adsorbent to form a complete monolayer on the surface bound at high C_e (mg.g^{-1}), and b is a constant, which accounts for the affinity of the binding sites (L mg^{-1}). q_m represents the limiting adsorption capacity, when the surface is fully covered with metal ions and helps in the evaluation of adsorption performance, particularly in cases, where the sorbent did not reach its full saturation during contact. From the plots between (C_e/q_e) and C_e the slope ($1/q_m$) and the intercept ($1/b q_m$) can be calculated. The linear Langmuir adsorption isotherms of Co^{2+} for the adsorbent obtained at different temperatures are given in Fig. 7.

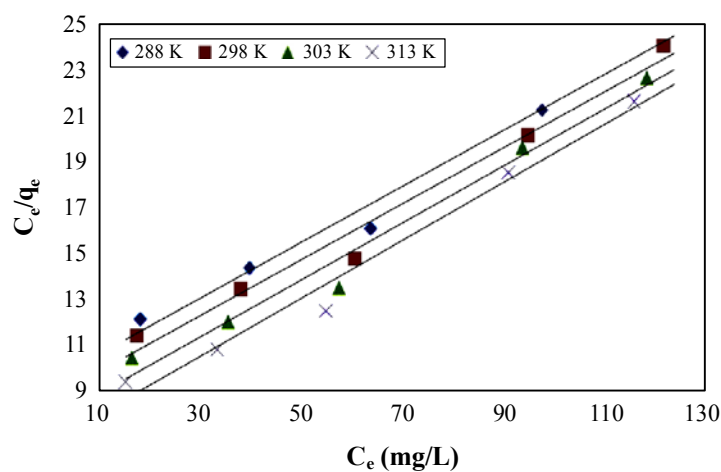


Fig. 7: Langmuir plot for biosorption of Co^{2+} on 3Å molecular sieves as biosorbent at various temperatures for biomass weight 20 g L^{-1} and at pH 5

Constant values at different metal ion concentrations was calculated and the values were shown in Table 1.

Table 1: Langmuir and Freundlich isotherm model parameters and R_L values at different initial metal ion concentrations for Co^{2+} adsorption by 3Å molecular sieves

Temp. (K)	Langmuir constants			Freundlich constants			Separation factor	
	q_m (mg/g)	B (L/mg)	R^2	k_f	n_f	R^2	C_T (mg/L)	R_L
288	8.183	0.0130	0.9850	0.2581	1.5862	0.9722	48.319	0.614
298	8.183	0.0141	0.9781	0.2783	1.6035	0.9632	96.34	0.422
303	8.032	0.0163	0.9775	0.3212	1.6600	0.9536	148.23	0.292
313	7.892	0.0188	0.9817	0.3724	1.7253	0.9495	197.5	0.211

Freundlich isotherm

Freundlich isotherm is the earliest known relationship describing the adsorption equation and is often expressed as:

$$q_e = K_f C_e^{\frac{1}{n_f}} \quad \dots(4)$$

Taking logarithm on both sides:

$$\log q_e = \log K_f + \frac{1}{n_f} \log C_e \quad \dots(5)$$

Where q_e is equilibrium adsorption capacity (mg g^{-1}), C_e is the equilibrium concentration of the adsorbate in solution, K_f and n_f are constants related to the adsorption process such as adsorption capacity and intensity, respectively. The plots in Fig. 8 show linearity for the isotherm drawn for adsorption of Co^{2+} onto 3Å molecular sieves and fitted well at various temperatures.

Adsorption kinetic models

The study of adsorption kinetics is very useful for understanding the involved mechanisms and also for the design of future large scale adsorption facilities. Many models are used to fit the kinetic adsorption experiments. The most used ones are the pseudo-first

order, pseudo-second order¹¹. In order to examine the mechanism of adsorption process such as mass transfer and chemical reaction, a suitable kinetic model is needed to analyze the rate data. Most models used in the literature have been extensively applied in batch reactors to describe the transport of adsorbates inside the adsorbent particles. All constants were calculated from the intercept and slope of the line obtained from linearized form of models. The equations corresponding to each model and their linearized forms, plots, slopes and intercepts are presented in Table 2.

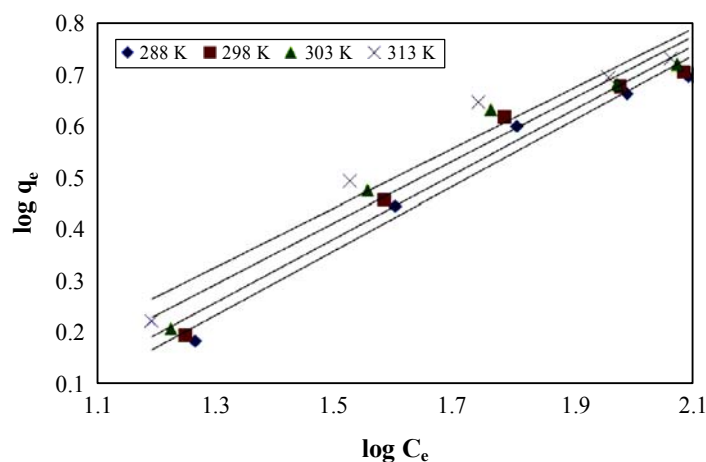


Fig. 8: Freundlich plot for biosorption of Co²⁺ over 3Å molecular sieves at different temperatures for biomass weight 20 g/L and at pH 5

Pseudo-first order/Lagergren kinetic model

The pseudo-first order or Lagergren kinetic rate equation for the adsorption of liquid-solid system was derived based on solid adsorption capacity. It is one of the most widely used adsorption rate equations for adsorption of a solute from a liquid solution. The pseudo-first order kinetic equation can be expressed as:

$$\frac{dq}{dt} = k_1(q_e - q_t) \quad \dots(6)$$

After integration and applying the boundary conditions, for $q_t = 0$ at $t = 0$ and $q_t = q_t$ at $t = t$, the integrated form of Eq. (6) becomes:

$$\log(q_e - q_t) = \log q_e - k_1 t \quad \dots(7)$$

Where q_e and q_t are the amounts of phosphates sorbed at equilibrium and at time t (mg g^{-1}), respectively, and k_1 is the rate constant of pseudo-first order sorption (L min^{-1}).

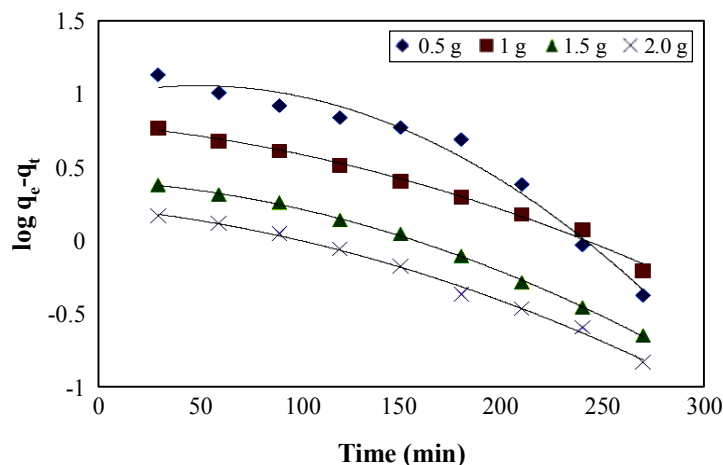


Fig. 9: First order kinetic plot for adsorption of metal ion (Co^{2+}) at 25°C , C_0 50 mg L^{-1} and pH 5

Pseudo-second order kinetic model

In view of the above, the fitness of the sorption data was tested using pseudo-second order reaction model. The pseudo-second order reaction model could be expressed by the rate expression as :

$$\frac{dq}{dt} = k_2(q_e - q_t)^2 \quad \dots(8)$$

On integration for boundary conditions when $t = 0$ to $t > 0$ and $q_t = 0$ to $q_t > 0$ and further simplifications, Eq. (8) becomes:

$$\frac{t}{q_t} = \frac{1}{k_2 q_e^2} + \frac{1}{q_e} t \quad \dots(9)$$

The plot of t/q_t vs. t (Fig. 10) of Eq. (9) gave a linear relationship from which the q_e and k_2 values were determined. The rate constants and the correlation coefficients for pseudo-second order kinetic model were calculated and summarized in Table 2. These values showed that the pseudo-second order kinetic plots fit well the adsorption data of cadmium metal for the adsorbent.

This kinetic model can be proposed to predict the kinetics of adsorption of Co^{2+} on 3\AA molecular sieves.

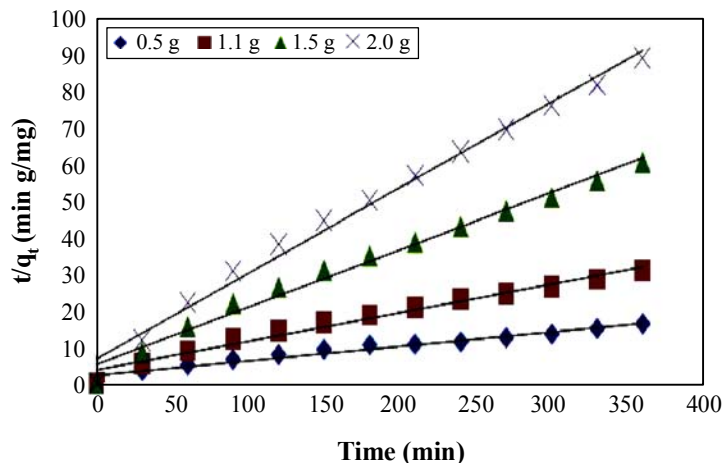


Fig. 10: Second order kinetic plot for adsorption of metal ion (Co^{2+}) at 25°C , C_0 50 mg L^{-1} and pH 5

Thermodynamic parameters and their determination

Thermodynamic parameters Gibbs free energy ΔG° is the basic criterion for deciding whether the chemical process does occur/proceed or not. The spontaneity of the reaction can also be judged by the sign and magnitude of ΔG° . A negative sign for ΔG° is an indicative of the spontaneity of any chemical process. To design any chemical process system, one should have the knowledge of changes that are expected to occur during chemical reaction. The rate and extent of changes are more informative in the design of process equipment. In view of the above, analysis has been carried out on the effect of thermodynamic parameters on the adsorption of Co^{2+} on 3\AA molecular sieves. The thermodynamic parameters such as changes in standard free energy change ΔG° , enthalpy ΔH° , and entropy ΔS° for any given adsorption process could be determined from the Equation:

$$\Delta G^\circ = -RT \ln K_C \quad \dots(10)$$

where ΔG° , is the free energy change, expressed as J mol^{-1} and b is the Langmuir equilibrium constant for the process. The values of b (Table 1) at different temperatures were processed according to the following Van't Hoff equation.

$$\log \frac{C_{ad}}{C_e} = -\frac{\Delta H^\circ}{2.303 RT} + \frac{\Delta S^\circ}{2.303 R} \quad \dots(11)$$

where b is in $L\ mg^{-1}$ and R is universal gas constant ($8.314\ J/mol.K$) The enthalpy changes (ΔH°) and entropy changes (ΔS°) for the adsorption process of Co^{2+} using 3\AA Molecular sieves were obtained from the plot of $\log \frac{C_{ad}}{C_e}$ drawn against $1/T$ (Fig. 11) and were compiled in Table 3. The positive value for ΔG° indicates the spontaneity of adsorption process. The positive ΔH° values indicated endothermic nature of the adsorption. The negative value of ΔS° suggested a decrease in the randomness at solid/solution interface during the adsorption of Co^{2+} ions on to 3\AA molecular sieves.

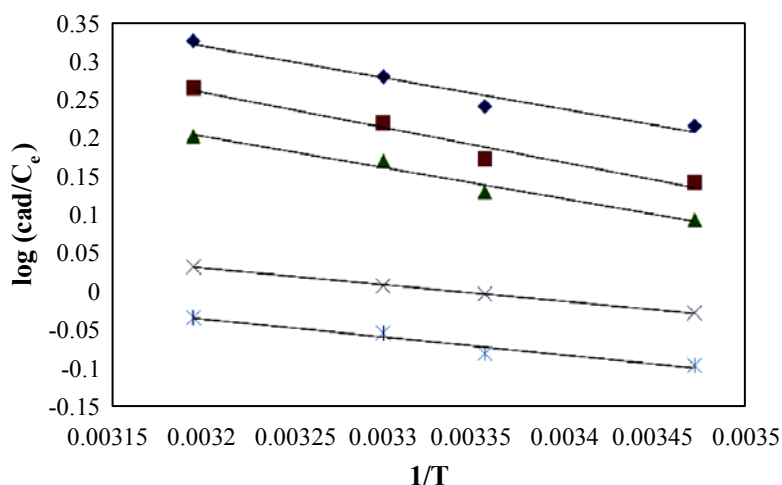


Fig. 11: Vant Hoff plot for adsorption of Co^{2+} over 3\AA molecular sieves as adsorbent plotted $\log C_{ad}/C_e$ vs $1/T$ at different total metal ion concentration using $20\ g\ L^{-1}$ adsorbent at pH 5

Table 2: Kinetic parameters for Co^{2+} adsorption on 3\AA molecular sieves

W ($g\ L^{-1}$)	K_2 ($gmg^{-1}\ min^{-1}$)	q_e ($mg\ g^{-1}$)	q_e (exp) $mg\ g^{-1}$	R^2
5	0.0004	27.932	3.6926	0.9839
10	0.0011	13.531	2.6452	0.9908
15	0.0031	6.702	2.0309	0.9934
20	0.0055	4.456	1.6582	0.9953

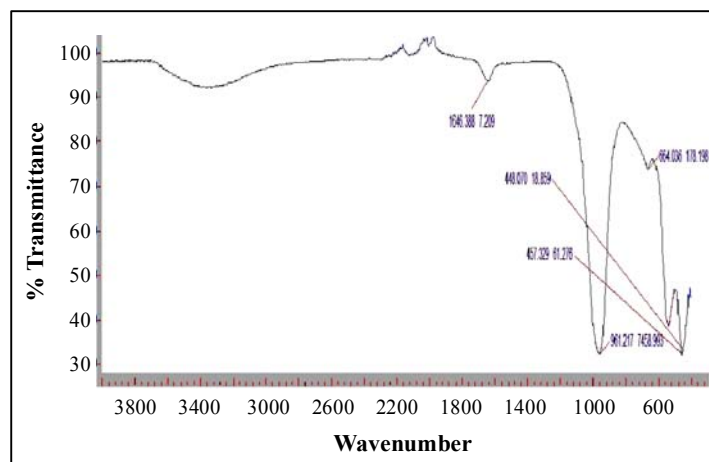
Table 3: Thermodynamic parameters for Co²⁺ adsorption 3Å molecular sieves

C ₀ (mg L ⁻¹)	ΔH ⁰ (kJ mol ⁻¹)	ΔS ⁰ (J mol ⁻¹ K)	ΔG ⁰ (kJ mol ⁻¹)	Temp. (K)
48.319	7.9341	31.5315	-9.0731	288
96.34	8.7883	33.0460	-9.8389	298
148.23	7.8026	28.8432	-8.7317	303
197.5	4.1068	13.7189	-4.2899	313
223.1	4.5085	13.7380		

Biomass characterization

Fourier transform infra-red spectroscopy analysis

The FTIR differences of spectra in pure 3Å molecular sieves adsorbent were compared to the spectra obtained in metal ion loaded 3Å molecular sieves to determine whether the observed differences are due to interaction of the metals ions with functional groups. The band positions of pure 3Å molecular sieves and loaded with Co²⁺ was shown in Table 4. The broad band at 3325.98 cm⁻¹ was shifted to 3387.22 and 3400.17 cm⁻¹ in Co²⁺. The significant involvement of the –OH stretching vibrations in the adsorption process was observed in all the three cases. –C≡C– is also involved in the adsorption process, as indicated by shifting of pure 3Å molecular sieves peak from 2120.56 to 2154.10 for Co²⁺ (Fig. 12 and 13).

**Fig. 12: FT-IR Spectrum of unloaded 3Å molecular sieves**

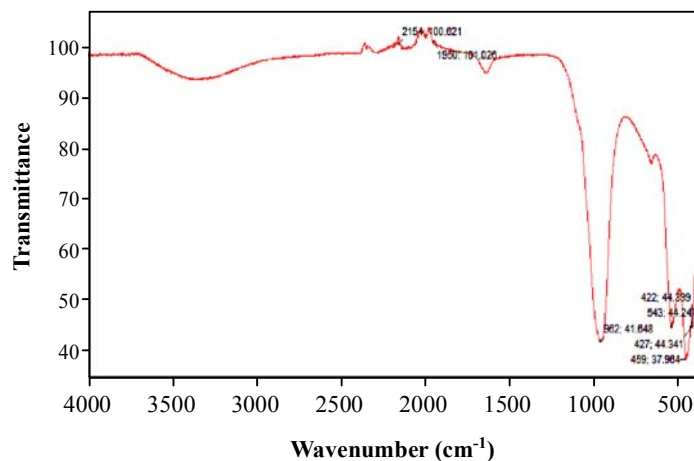


Fig. 13: FT-IR spectrum of Co²⁺ loaded 3Å molecular sieves

Characterization of 3 Å molecular sieves using SEM studies

The SEM images were taken by applying 10 kV voltage with different magnification times for the clarification of surface. The SEM micrographs of 3Å molecular sieves powder before and after adsorption were studied and are depicted in Figs. 14 and 15 for unloaded 3Å molecular sieves and for loaded 3Å molecular sieves with Co²⁺, respectively.

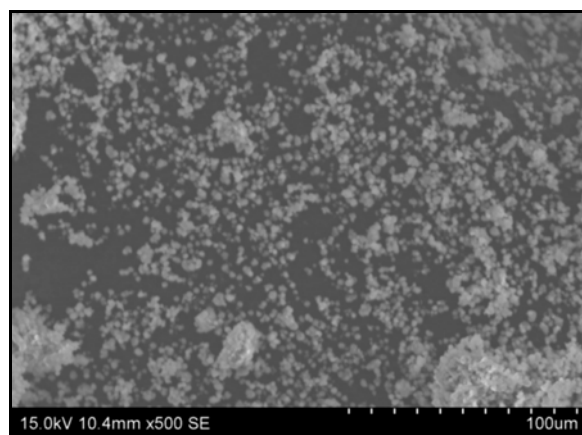


Fig. 14: SEM of powder 3Å molecular sieves without metal ions

It is evident from analysis that the surface area of 3Å molecular sieves are uneven, heterogeneous with pores on the surfaces. SEM image of pure 3Å molecular sieves shows number of pores with different diameters and different pore areas. The change in

morphology indicates the accumulation of liquid phase concentration of charge moieties onto 3Å molecular sieves surface areas.

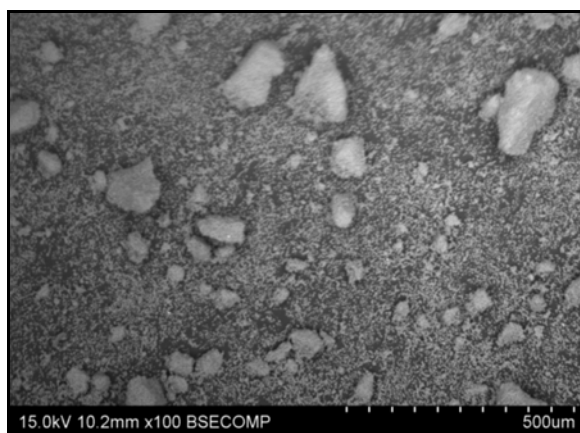


Fig. 15: SEM of powder 3Å molecular sieves loaded with Co²⁺ ions

Table 4: Band positions of pure 3Å molecular sieves and loaded with Co²⁺

S. No.	Band shift position, cm ⁻¹		Description
	Un loaded biomass	Loaded with Co ²⁺	
1	3325.98	3387.22	Corresponding to the OH-stretching vibration
2	2120.56	2154.10	-C≡C stretch, alkynes
3	1646.38	1638.97	Stretching and angular deformation of the hydroxyl of water of hydration
4	961.21	962.41	AlO bending vibration
5	664.03	670.58	Si-O symmetric stretching
6	535.98	543.44	AlOSi skeletal vibrations

CONCLUSION

The equilibrium time for Co²⁺ on 3Å molecular sieves was 5½ hrs. The optimum pH was observed at 5 where maximum adsorption was observed. The increase in total Co²⁺ concentration from 48.75 to 223.14 mg L⁻¹ decreased the percent of removal from 68.02% to

47.12%. The adsorption capacity (q_e) is 6.702 mg g^{-1} . The amount of Co^{2+} adsorbed increases with an increase in adsorbent dosage from 5 to 20 g L^{-1} . The optimum temperature for adsorption on 3\AA molecular sieves is 25°C . Langmuir equilibrium isotherm model proved to be good fit for the experimental data of Co^{2+} adsorption on 3\AA molecular sieves. The kinetics of the adsorption of Co^{2+} has been described by a pseudo second-order kinetic model with R^2 0.999. Free energy change (ΔG^0) with negative sign reflects the feasibility and spontaneous nature of the process.

REFERENCES

1. K. Adan, B. Syed and A. Claudio, Biosorption of Some Toxic Metal Ions by Chitosan Modified with Glycidylmethacrylate and Diethylenetriamine, *Chem. Engg. J.*, **171**, 159-166 (2011).
2. G. W. Stratton, In Review in Environmental Toxicology (Ed. Hodgson. E.) Elsevier, Amsterdam (1987) pp. 85-94.
3. S. Rengaraj and S. H. Moon, Kinetics of Adsorption of Co (II) Removal from Water and Wastewater by Ion Exchange Resins, *Water Res.*, **36**, 1783-1793 (2002).
4. S. Zhang, Z. Guo, J. Xu, H. Niu, Z. Chen and J. Xu, Effect of Environmental Conditions on the Adsorption of Radiocobalt from Aqueous Solution to Treated Eggshell as Biosorbent, *J. Radioanal. Nucl. Chem.*, **288**, 121-130 (2010).
5. C. K. Hersh, Molecular Sieves, Reinhold Publishing Corporation (1961).
6. R. Leyva-Ramos, J. R. Rangel-Mendez, J. Mendoza-Barron, L. Fuentes-Rubio and R. M. Guerrero-Coronado, Adsorption of Cadmium (II) from Aqueous Solution Onto Activated Carbon, *Water Sci. Technol.*, **35(7)**, 205-211 (1997).
7. G. Suraj, C. S. P. Iyer and M. Lalithambika, Adsorption of Cadmium and Copper by Modified Kaolinites, *Appl. Clay Sci.*, **13**, 293-306 (1998).
8. S. Dhabhi, M. Azzi, N. Saib, M. de la Guardia, R. Faure and R. Durand, Removal of Trivalent Chromium from Tannery Waste Waters using Bone Charcoal, *Anal. Bioanal. Chem.* **374**, 540-546 (2002).
9. F. Fang, L. Kong, J. Huang, S. Wu, K. Zhang, X. Wang, B. Sun, Z. Jin, J. Wang, X.-J. Huang and J. Liu, Removal of Cobalt Ions from Aqueous Solution by an Amination Grapheme Oxide Nanocomposite, *J. Hazard. Mater.*, **270**, 1-10 (2014).

10. M. Sekar, V. Sakthi and S. Rengaraj, Kinetics and Equilibrium Adsorption Study of Lead (II) Onto Activated Carbon Prepared from Coconut Shell, *J. Coll. Interface Sci.*, **279**, 307-313 (2004).
11. K. Riahi, S. Chaabane and B. B. Thayer, A Kinetic Modeling Study of Phosphate Adsorption Onto Phoenix Dactylifera L. Date Palm Fibers in Batch Mode, *J. Saudi Chem. Soc.*, doi: 10.1016/j.jscs.2013.11.007 (2013).

Revised : 09.10.2015

Accepted : 11.10.2015